16th World Conference on Earthquake Engineering, 16WCEE 2017
Santiago Chile, January 9th to 13th 2017
Paper N° 4425
Registration Code: S-N1461963002

STRONG GROUND MOTION SIMULATION OF THE 2015 ILLAPEL EARTHQUAKE USING CORRECTED EMPIRICAL GREEN'S FUNCTIONS

C. Fernández[(1)], P. Aguirre[(2)], J.C. De la Llera[(3)], G. Candia[(4)], A. Nozu[(5)]

[(1)] PhD Candidate, Department of Structural and Geotechnical Engineering and National Research Center for Integrated Natural Disaster Management (CIGIDEN) CONICYT/FONDAP/15110017, Pontificia Universidad Catolica de Chile, cfernandez@ing.puc.cl
[(2)] Adjunct Assistant Professor, School of Engineering and National Research Center for Integrated Natural Disaster Management (CIGIDEN) CONICYT/FONDAP/15110017, Pontificia Universidad Catolica de Chile, paula.aguirre@cigiden.cl
[(3)] Professor, Department of Structural and Geotechnical Engineering and National Research Center for Integrated Natural Disaster Management (CIGIDEN) CONICYT/FONDAP/15110017, Pontificia Universidad Catolica de Chile, jcllera@ing.puc.cl
[(4)] Assistant Professor, Universidad del Desarrollo and National Research Center for Integrated Natural Disaster Management (CIGIDEN) CONICYT/FONDAP/15110017, gcandia@udd.cl
[(5)] Director of Earthquake Disaster Prevention Engineering Division, Port and Airport Research Institute, Yokosuka, Japan, nozu@pari.go.jp

Abstract

The September 16th 2015 Illapel, Chile, earthquake (M_w 8.4) generated a good set of aftershock data that enabled us to develop and to validate a model for synthetic ground motion generation. This study presents a methodology to generate strong ground motions based on site amplification and phase characteristics of seismic waves, and also based on a source model that was newly developed for the earthquake. The methodology includes the superposition of corrected empirical Green's functions that consider the three effects: source, path and site. The path effects incorporate the attenuation of seismic waves between the source and the recording stations, and include both geometric spreading and inelastic attenuation. Weak motion data obtained at the strong-motion stations was used to evaluate empirical site amplification factors. For this purpose, aftershocks recorded during the first three months after the main shock were used. Furthermore, the phase characteristics of the Green's functions were determined based on the weak motion data recorded at the stations. The source model involves two SPGAs (strong-motion pulse generation areas). The locations of the SPGAs were basically determined based on the arrival times of the velocity pulses. The SPGA sizes were chosen according to the pulse duration. The methodology was validated using observed records in terms of velocity waveforms and Fourier spectra. According to the results, the velocity waveforms including pulses were well reproduced in a frequency range of interest to structural engineering (0.2 to 1 Hz). The agreement between the simulated and measured waveforms makes this model a strong platform to assess hazard at specific sites where detailed hazard assessment is required.

Keywords: strong ground motion, Illapel earthquake, corrected empirical Green's functions, site effects.

1. Introduction

Prediction of strong ground motions is an important step to mitigate risks and to prevent disasters in countries with great earthquake activity, and the development of methodologies that can accurately simulate strong ground motions is an important issue. The authors are especially interested in developing methodologies that can be used to assess seismic hazard at specific sites where engineered structures will be constructed and detailed hazard assessment is required. For such purposes, methodologies that are applicable for simulating time history of strong ground motions especially in the frequency range relevant to structural damage should be developed. Development and validation of such methodologies have not necessarily been sufficient for Chilean subduction earthquakes so far.

On September 16th 2015, the central zone of Chile was affected by a M_w 8.4 subduction earthquake at 22:54:28 UTC, with an epicenter (31.553° S, 71.864° W) located nearly 48 km west of Illapel city (hereafter referred to as the "Illapel earthquake"). The rupture zone was estimated to be 640 km along strike with the strike angle of 4°, and 168 km along dip with the dip angle of 19° [1], and it produced strong ground motions characterized by the existence of at least one clear pulse recorded at strong-motion stations near the epicenter. The earthquake was followed by numerous aftershocks that generated an excellent set of weak motion data, which, together with the main shock records, enabled us to develop and to validate a model for synthetic ground motion generation.

In this study, the authors considered applying a method that is based on empirical site amplification and phase characteristics [e.g., 2, 3, 4, 5] to the Illapel earthquake, because the method was applied to past large subduction earthquakes including the 2011 Tohoku earthquake (M_w 9.0) [6, 7] and, when it was combined with appropriate source models, it successfully reproduced velocity waveforms and its pulses, especially over the frequency range relevant to structural damage.

The details of the method are described in the next chapter, but the essence can be summarized as follows. Generally speaking, strong ground motions are generated by three combined effects: source effect, path effect and site effect. In this methodology, first, ground motions from a small event (i.e., Green's functions) are evaluated. The Fourier amplitude spectrum of the Green's function is evaluated as a multiplication of the source, path and site effects. The source spectrum is assumed to follow the ω-square model developed by Aki in 1967 [8]. The path effect is modeled taking into account both geometrical spreading and inelastic attenuation of seismic waves [9]. In this particular application to the Illapel earthquake, the path model developed by Satoh and Tatsumi [10] for Japanese earthquakes was revised and used as will be explained later. The site effect can be defined as the influence of sediments on strong ground motions and it includes the amplification of body waves and generation and propagation of basin-induced surface waves. In this article, both path and site effects were evaluated based on weak motion records at several stations. These three effects are considered to calculate the Fourier amplitude spectrum of the Green's function and weak motion records are used for adding phase information. Finally, the Green's functions are superposed by using Irikura's technique [11, 12, 13] considering time-shift of body waves.

A source model for the Illapel earthquake was newly developed for the simulation. The source model involves two SPGAs (strong-motion pulse generation areas). The locations of the SPGAs were basically determined based on the arrival times of the velocity pulses. The SPGA sizes were chosen according to the pulse duration.

By combining the simulation methodology and the source model, strong motion simulation for the Illapel earthquake was conducted and the methodology was validated using observed records especially for the frequency range from 0.2 to 1 Hz, because strong motions in this frequency range have significant effects on a wide range of engineered structures like buildings and port structures.

2. Methodology

The first step is to evaluate ground motions from a small event, i.e., Green's functions. In the frequency domain, a Green's function can be written as follows:

$$\left|S(f)\right|\cdot\left|P(f)\right|\cdot\left|G(f)\right|\cdot\frac{O_s(f)}{\left|O_s(f)\right|_p} \tag{1}$$

where $|S(f)|$ corresponds to the source spectrum that follows the ω-square model, $|P(f)|$ represents the path effect which is the attenuation of seismic waves due to geometrical spreading and inelastic attenuation, $|G(f)|$ corresponds to the site amplification factor, $O_s(f)$ is the Fourier transform of a record at the site and $\left|O_s(f)\right|_p$ is its Parzen-windowed amplitude (a band width of 0.05 Hz was used to smooth the spectra). Then, the first three terms of Equation (1) represent the Fourier amplitude of the Green's function, and the last quotient determines the Fourier phase of the Green's function.

The second step is to superpose Green's functions to obtain strong ground motions from a large event (or a subevent of a large event) using a superposition method similar to Irikura's Empirical Green's Functions (EGF) method [13]. Irikura's EGF method is designed so that, if it is applied to a Green's function that follows the ω-square model, the synthetic ground motion also basically follows the ω-square model. Thus, the synthetic ground motion obtained based on the present methodology basically follows the ω-square model.

The original EGF method and the present method are compared in Table 1. The Fourier phase of the Green's function and the superposition method are common between the two methods. The only difference is the Fourier amplitude of the Green's function. Therefore, the present method can be redefined as the EGF method with a Green's function whose source spectrum is corrected to follow the ω-square model. Therefore, the present method is referred to as the "corrected EGF method" in this article.

Table 1 – Comparison between the original and corrected EGF methods

	Original EGF method	Corrected EGF method (present method)
Fourier amplitude of Green's function	Weak motion records	S(f)×P(f)×G(f)
Fourier phase of Green's function	Weak motion records	Weak motion records
Superposition(ΣΣΣ)	Irikura et al. (1997)	Irikura et al. (1997)

2.1 Source model

It has been revealed that the radiation of seismic energy from a large subduction earthquakes is quite frequency dependent [e.g., 14], i.e., strong ground motions relevant to structural damage are not necessarily radiated from a large slip region. In terms of Chilean subduction earthquakes, Okuwaki et al. [15] argues that high frequency (0.5-2 Hz) energy radiation preceded the rupture of asperities for the 2010 Maule earthquake (M_w8.8). For the Illapel earthquake, Okuwaki et al. [16] suggests that the largest slip episode was triggered by a strong high-frequency (0.3-2 Hz) radiation event at the down-dip edge of the fault. These studies about high-frequency radiation are quite insightful, although these studies themselves are not intended to propose a source model that can be used to simulate strong ground motions.

In this study, to simulate strong ground motions, an SPGA model was newly developed for the Illapel earthquake. The SPGA model can be defined as a source model composed of subevents whose sizes are determined referring to the duration of velocity pulses observed at near-source stations. The subevents determined in this way are referred to as the SPGAs (strong-motion pulse generation areas). SPGA models have been developed for past large subduction earthquakes including the 2011 Tohoku earthquake (M_w 9.0) [6, 7] and successfully reproduced strong ground motions including velocity pulses in the frequency range relevant to structural damage, when they were combined with the corrected empirical Green's function method.

For the Illapel earthquake, two SPGAs were modeled to reproduce velocity pulses and waveforms at five near-source stations. The stations belong to the CSN (Centro Sismológico Nacional) and the records are available at CSN's webpage [17]. SPGAs were located based on the analysis of pulse arrival times. Alternatively, they could be located based on HBP/BP analyses. Figure 1 shows the location of the epicenter of earthquake, the names and locations of the target stations where velocity waveforms were reproduced, and the locations of the two SPGAs. Properties and exact location assigned to each SPGA are shown in Table 1 (from left to right: latitude, longitude, depth, length, width, rupture time, rise time and seismic moment) and they were selected to well reproduce the pulses at the stations. It is interesting to note that both SPGAs are located close to the high-frequency radiation events determined by Okuwaki and Yagi [16].

Table 2 – Properties assigned to the SPGAs

	Lat (deg)	Lon (deg)	Depth (km)	L (km)	W (km)	t_{rup} (s)	t_{ris} (s)	M_0 (dyn-cm)
SPGA 1	-31.547	-71.448	39.4	2.0	2.0	9.0	0.17	5.00E+25
SPGA 2	-31.400	-71.250	46.0	4.0	2.5	31.5	0.21	2.00E+26

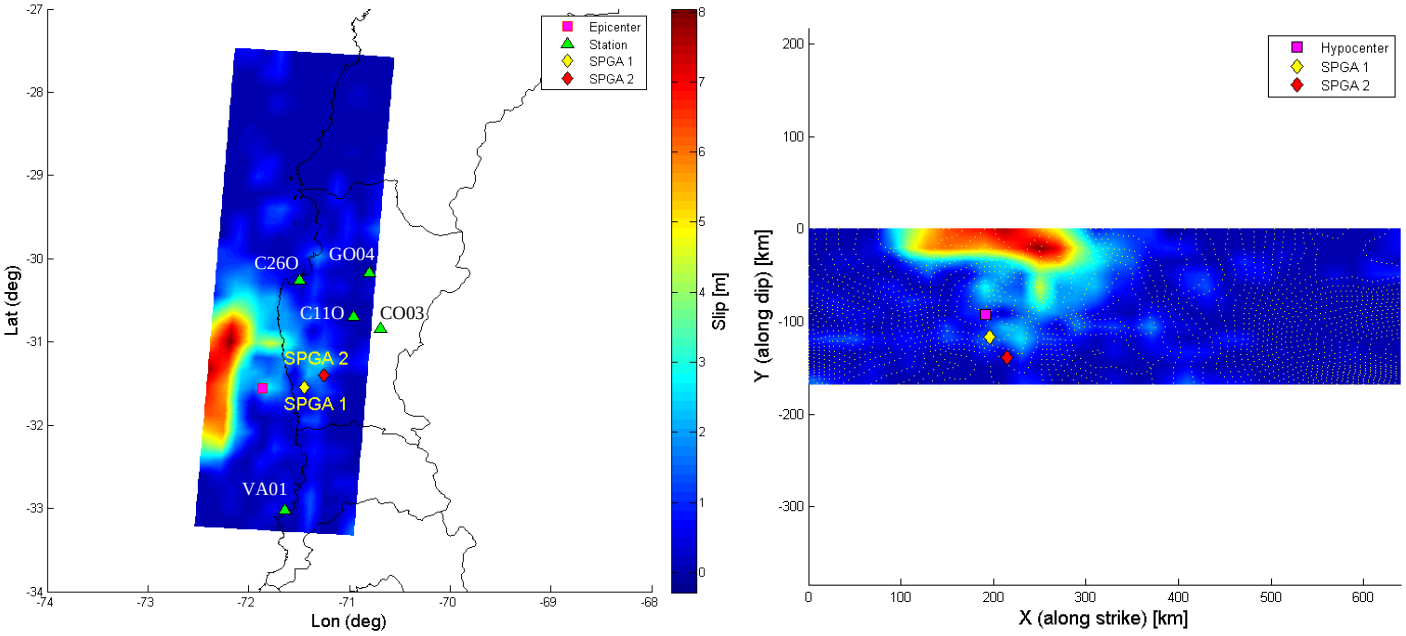

Fig. 1 − (left) Rupture zone, slip distribution, epicenter location, SPGA locations and target stations plotted on the map. (right) Fault plane, slip distribution, hypocenter location (11.1 km deep) and SPGA locations in a coordinate system with the X and Y axes pointing in the strike and dip directions, respectively. Dotted contour lines represent the rupture time.

Fig. 2 shows the radial propagation of the pulse generated upon the rupture of SPGA 2 (22:54:59.5 UTC) through the stations, with an averaged S-wave velocity of 4.4 km/s. In Fig. 2, t=0 is the rupture time at the hypocenter (22:54:28 UTC).

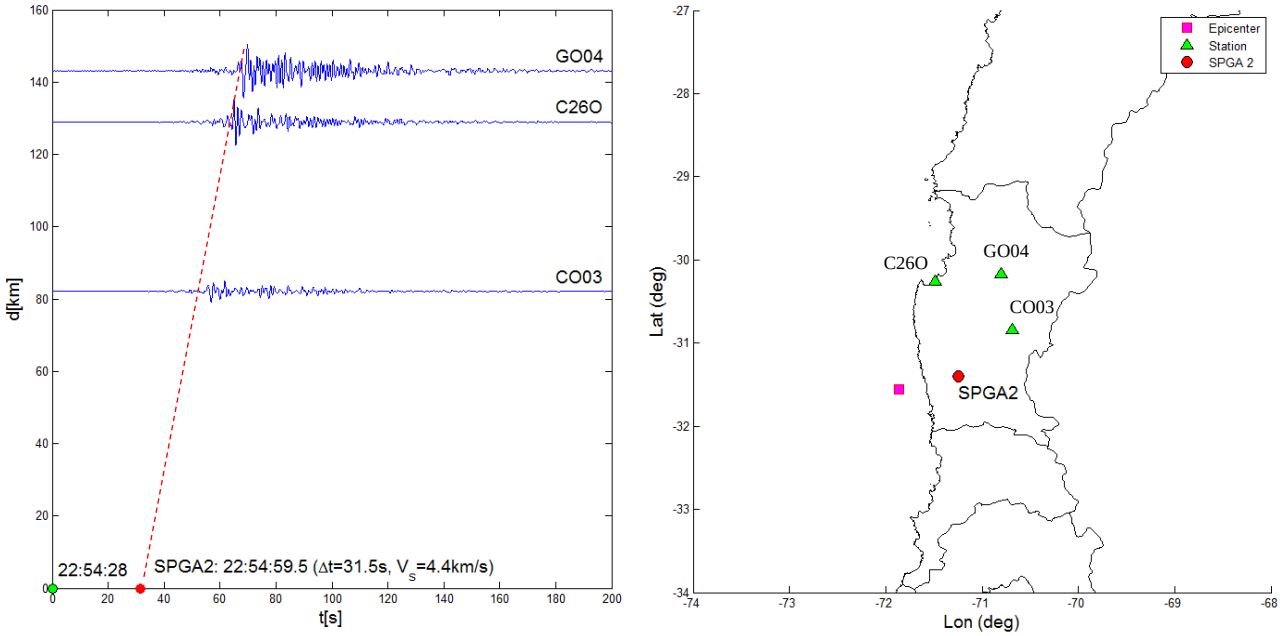

Fig. 2 – (left) Radial propagation of the pulse from SPGA 2 to stations CO03, C26O and GO04. (right) Location of stations CO03, C26O, GO04 and SPGA 2.

2.2 Path and site effects

Path effect represents the attenuation of seismic waves from the source to the site. The expression used in the present method was first proposed by Boore [9] and modified by Satoh and Tatsumi [10] to consider smaller attenuation at large distances as follows:

$$P(r,f)=\frac{1}{R(r)}\exp\left[-\frac{\pi f r}{Q(f)V_s}\right] \tag{2}$$

where

$$R(r)=\begin{cases} r & r\le 80\,km \\ (80r)^{0.5} & r>80\,km \end{cases} \tag{3}$$

A generalized inversion technique [e.g., 18] was applied to the weak motion records to evaluate both path and site effects empirically. The method is based on the following linear equation:

$$\log|O_{ij}|=\log|S_i|+\log|P_{ij}|+\log|G_j| \tag{4}$$

where $|O_{ij}|$ is the observed Fourier spectrum (vector sum of two horizontal components), $|S_i|$ is the source effect for the i-th earthquake, $|P_{ij}|$ is the path effect and $|G_j|$ is the site amplification factor at the j-th site. Since the path effect is a product of the geometrical spreading term $1/R(r)$ and the inelastic attenuation term $\exp\{-\pi f r/[Q(f)V_s]\}$, the unknown term is actually the exponent of the exponential function. A uniform Q value was assumed for the target region. As a result, Equation (4) involves M+N+1 unknown parameters, where

M stands for the number of earthquakes and *N* stands for the number of stations. Using a sufficient number of weak motion records, the unknown parameters can be estimated using a linear regression analysis. In the present analysis, *M*=41 and *N*=30. The number of the records was 307. However, this methodology needs another constraint, that is, it is necessary to constrain at least one source spectrum or one site amplification factor. One common practice is to assume a site amplification factor equal to one for all frequencies for a rock site. In this research, the site amplification factor was assumed to be equal to one at VA01 station, because the station exhibited the smallest site amplification factor among all the stations used.

The quality factor $Q(f)$ was estimated for each frequency and was regressed to a linear equation as shown in Fig. 3. The result was a quality factor given by

$$Q(f) = 239 f^{0.71} \tag{5}$$

The site amplification factors were calculated for 30 stations that recorded the Illapel mainshock. Fig. 4 shows the site amplification factors for the target stations C11O, GO04, CO03 and C26O shown in Fig.1. The site amplification factor for VA01 is not shown because it was assumed to be one (i.e. there is no amplification due to site effects at this station).

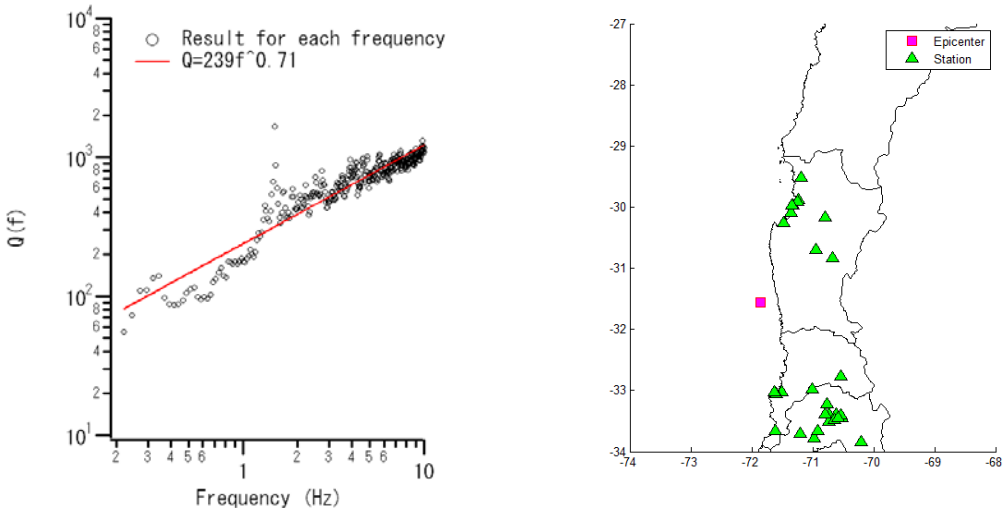

Fig. 3 – (left) Q value in log-log scale determined using a generalized inversion technique with 30 stations and 307 records. (right) Locations of 30 stations used for the analysis.

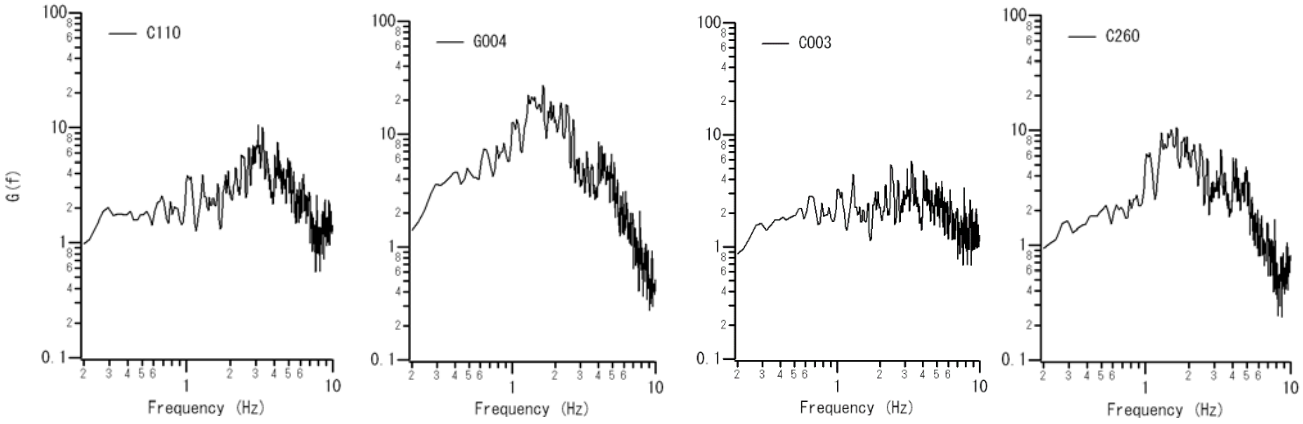

Fig. 4 – Site amplification factors for the target stations C11O, GO04, CO03 and C26O (from left to right)

3. Results

The methodology presented in the former sections was applied and synthetic ground motions were generated for the stations C11O, GO04, CO03, C26O and VA01. For this calculation, the parameter *PRTITN* [9], which represents the partition of S-wave energy into two horizontal components, was assumed to be 0.71 (equal distribution of energy between N-S and E-W components) for all the stations, except for the station VA01 near Santiago, where 0.85 for the E-W component and 0.53 for the N-S component were used to be consistent with the observed data. Phase characteristics of the corrected empirical Green's functions were taken from the weak motion data recorded at the stations. Table 3 summarizes the aftershocks selected to obtain phase characteristics at each station.

Fig. 5 and Fig. 6 compare the observed and synthetic velocity waveforms in the frequency range between 0.2 and 1 Hz at these stations. Fig. 7 and Fig. 8 compare the observed and synthetic acceleration spectra at the same stations.

As shown in Fig. 5 and Fig. 6, the observed pulses in the frequency range between 0.2 and 1 Hz are, in general, well reproduced. For the station C11O in its E-W component, the pulse that arrives at approximately 90 s is very well reproduced. In the N-S component the pulse is well reproduced too, but the synthetic waveform has a positive peak that is overestimated. Nevertheless, it generates a positive value of peak ground velocity almost equal to the negative one, it could only have a minor effect as long as the resultant waveform is intended to be used for the design of structures. The same thing occurs at the station GO04, where in general the pulse is fairly well reproduced.

At the station CO03, the synthetic waveforms overestimate the amplitude of the pulse that arrives approximately at 60 s. However, the shape and the duration of the pulse seem to be correct. Since the durations of the velocity pulses are related to the sizes of the SPGAs that generate them, this result might be indicating the accuracy of the SPGA size (Table 2).

In the E-W component of the signal at the station C26O, the pulse amplitude is underestimated, but is well reproduced in the N-S component. As in the station CO03, the pulse in both components seems to be consistent with the observed one in terms of duration.

Finally, there are two important pulses at the station VA01. The first one arrives at approximately 60 s, and the second arrives at approximately 100 s. Both pulses are basically well represented by the synthetic velocity waveforms. Both the amplitude and duration are reproduced in the E-W component, but the amplitude is slightly overestimated in the N-S component. It is important to mention that a source model with two SPGAs was generated because of the two pulses involved in the observed velocity waveforms at the station VA01. A source model with only one SPGA can almost explain the observed waveforms at the stations located to the north of the epicenter probably because the effect of SPGA2 is so predominant at these stations, but it is necessary to include two SPGAs to explain the generation of two pulses at the station VA01.

Table 3 – Aftershocks used to add phase characteristics to the corrected EGF at each selected station

Station	Lat (deg)	Lon (deg)	Depth (km)	Date	Time (UTC)	M_L
C11O	-31.759	-71.737	40.7	2015-09-21	5:39:34	6.2
GO04	-31.759	-71.737	40.7	2015-09-21	5:39:34	6.2
CO03	-31.759	-71.737	40.7	2015-09-21	5:39:34	6.2
C26O	-31.461	-71.704	53.3	2015-09-17	3:55:15	5.8
VA01	-31.901	-71.899	29.2	2015-09-16	23:16:08	6.8

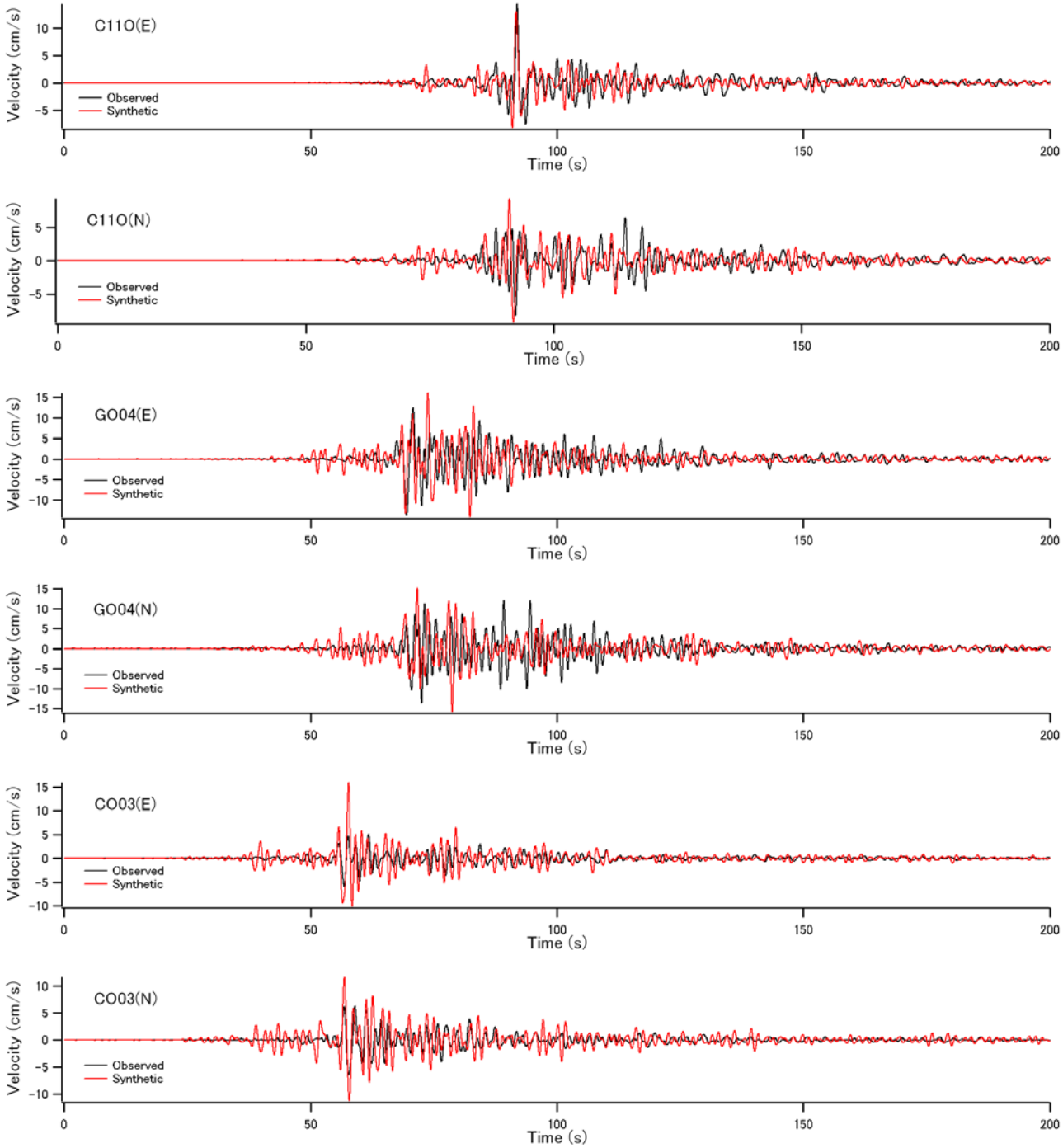

Fig. 5 – Observed and synthetic velocity waveforms (from 0.2 to 1 Hz) for the stations C11O, GO04 and CO03, N-S and E-W components.

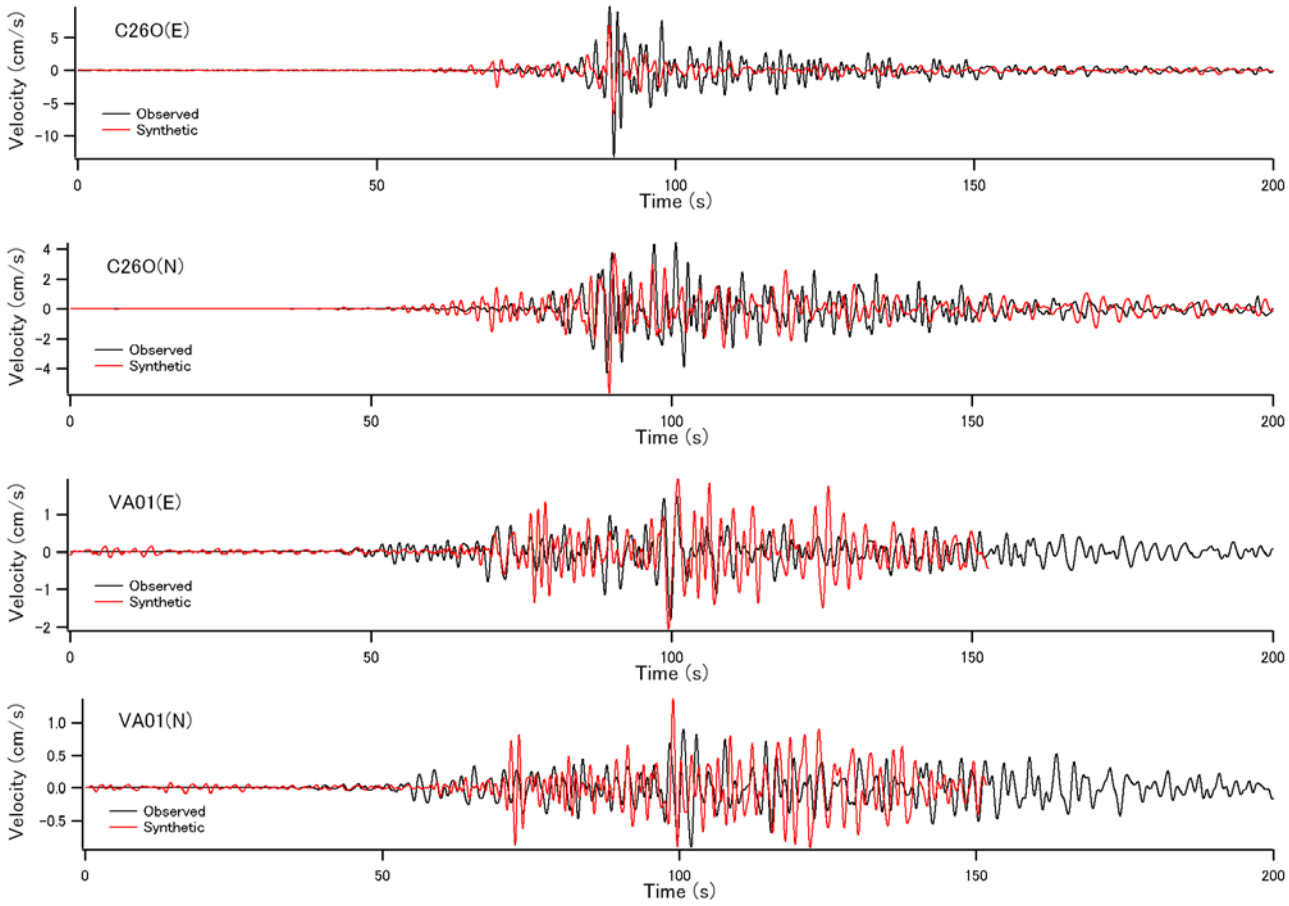

Fig. 6 – Observed and synthetic velocity waveforms (from 0.2 to 1 Hz) for the stations C26O and VA01, N-S and E-W components.

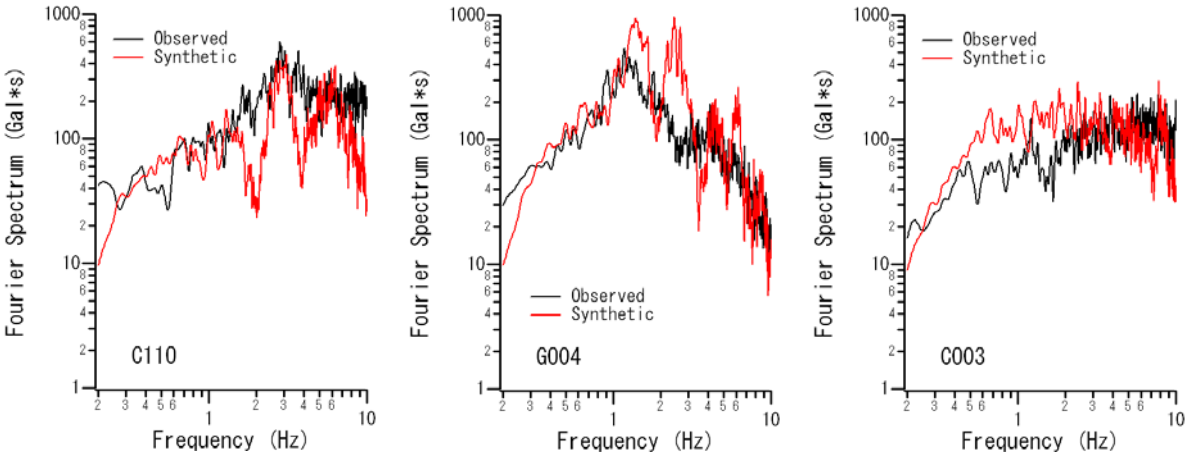

Fig. 7 – Observed and synthetic acceleration spectra at the stations C11O, GO04 and CO03 (vector sum of two horizontal components).

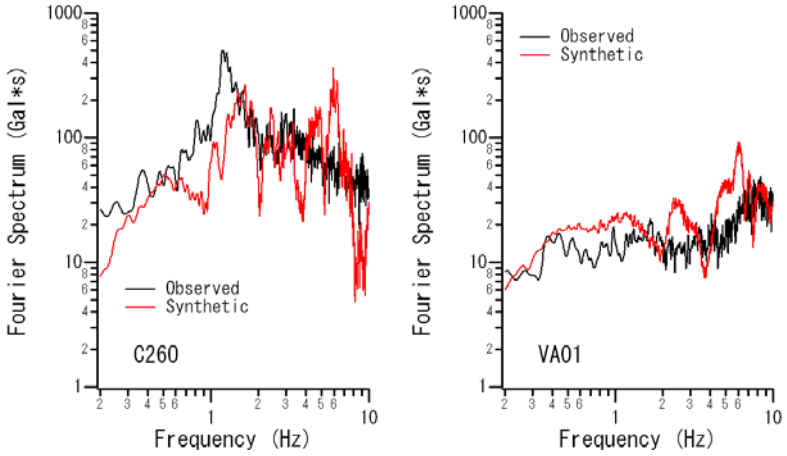

Fig. 8 – Observed and synthetic acceleration spectra at the stations C26O and VA01 (vector sum of two horizontal components).

4. Conclusions

In this study, simulation of strong ground motions were conducted for the 2015 Illapel earthquake (M_w 8.4) using the corrected empirical Green's function method, based on the empirical site amplification and phase characteristics. A source model for the earthquake was newly developed for the simulation. The source model involves two SPGAs (strong-motion pulse generation areas). The locations of the SPGAs were basically determined based on the arrival times of the velocity pulses. Both SPGAs are located close to the high-frequency radiation events suggested by Okuwaki et al. [16]. The SPGA sizes were chosen according to the pulse duration. A generalized inversion technique was applied to the weak motion records to evaluate both path and site effects empirically. By combining the simulation methodology and the source model, strong motion simulation for the Illapel earthquake was conducted and the methodology was validated using observed records especially for the frequency range from 0.2 to 1 Hz, because strong motions in this frequency range have significant effects on a wide range of engineered structures like buildings and port structures.

According to the results, the velocity waveforms including pulses were basically well reproduced in a frequency range of interest to structural engineering. The agreement between the simulated and measured waveforms makes this model a strong platform to assess hazard at specific sites where detailed hazard assessment is required.

The model used in this research could probably be improved to explain the data more accurately. Locations of the SPGAs could be more specific and some of other parameters could be improved to do a better representation of the observed waves. However, the model proposed in this article could serve as an approximated model that can explain main features of the observed records of the Illapel earthquake.

5. Acknowledgements

The authors would like to thank the Centro Sismologico Nacional (CSN) for providing the strong motion data. This database is available at CSN's webpage (www.sismologia.cl) for everybody who needs it.

6. References

[1] USGS website (URL: http://earthquake.usgs.gov/earthquakes/eventpage/us20003k7a#general)

[2] Kowada, A., Tai, M., Iwasaki, Y. and Irikura, K.: Evaluation of horizontal and vertical strong ground motions using empirical site-specific amplification and phase characteristics, *J. Struct. Constr. Eng*., AIJ, No.514, pp.97-104, 1998 (in Japanese with English abstract).

[3] Nozu, A., Nagao, T. and Yamada, M.: Simulation of strong ground motions based on site-specific amplification and phase characteristics, *Third Int. Symp. Effects of Surface Geol. on Seism. Motion*, Grenoble, France, 2006.

[4] Nozu, A. and Sugano, T.: Simulation of strong ground motions based on site-specific amplification and phase characteristics – accounting for causality and multiple nonlinear effects –, *Tec. Note of Port and Airport Res. Inst.*, No.1173, 2008 (in Japanese with English abstract)

[5] Nozu, A.: Prediction of strong ground motions from huge subduction earthquakes in the period range from 1-5 seconds, *Prog. and Abst., Seism. Soc. of Jap. 2010, Fall Meeting*, B12-04, 2010 (in Japanese).

[6] Nozu, A.: A super asperity model for the 2011 off the Pacific coast of Tohoku earthquake, *Journal of Japan Association for Earthquake Engineering*, Vol.14, 2014, pp.36-55.

[7] Nozu, A., Yamada, M., Nagao, T. and Irikura, K.: Generation of strong motion pulses during subduction earthquakes and scaling of their generation areas, *Journal of Japan Association for Earthquake Engineering*, Vol.14, 2014, pp.96-117.

[8] Aki, K.: Scaling law of seismic spectrum, *J. Geophys. Res*, Vol.71, 1967, pp.1217-1231.

[9] Boore, D.M.: Stochastic simulation of high-frequency ground motions based on seismological models of the radiated spectra, *Bull. Seism. Soc. of Am*, Vol.73, 1983, pp.1865-1894.

[10] Satoh, T. and Tatsumi, Y.: Source, path and site effects for crustal and subduction earthquakes inferred from strong motions records in Japan, *J. Struct. Constr. Eng.*, AIJ, No.556, pp.15-24, 2002 (in Japanese with English abstract).

[11] Irikura, K. (1983): Semi-empirical estimation of strong ground motions during large earthquakes, Bull. Disas. Prev. Res. Inst., Kyoto Univ., Vol.33, Part 2, No.298, pp.63-104.

[12] Irikura, K. (1986): Prediction of strong acceleration motions using empirical Green's function, Proceedings of the 7th Japan Earthquake Engineering Symposium, pp.151-156

[13] Irikura, K., T. Kagawa and H. Sekiguchi (1997): Revision of the empirical Green's function method by Irikura (1986), Seismological Society of Japan Fall Meeting, No.2, B25 (in Japanese)

[14] Koper KD, Hutko AR, Lay T, Ammon CJ and Kanamori H (2011): Frequency-dependent rupture process of the 2011 Mw9.0 Tohoku earthquake: Comparison of short period P wave backprojection images and broadband seismic rupture models. *Earth Planets Space*, **63**, 599-602.

[15] Okuwaki R., Yagi Y. and Hirano S. (2014): Relationship between high-frequency radiation and asperity ruptures, revealed by hybrid back-projection with a non-planar fault model, *Scientific Reports, |4:7120 DOI: 10.1038/srep07120*

[16] |Okuwaki R., Yagi Y., Aranguiz R., Gonzalez J. and Gonzalez G. (2016): Rupture process during the 2015 Illapel, Chile earthquake: zigzag-along-dip rupture episodes, *Pure Amml. Geophys. DOI 10.1007/s00024-016-1271-6*

[17] CSN webpage (URL: www.sismologia.cl)

[18] Iwata T., Irikura K. (1986): Separation of source, propagation and site effects from observed S waves. *Zisin*, **39,** 579-593 (in Japanese with English abstract).